Density-Based Control of Air Coolers in Supercritical CO_2 Power Cycles ⋆

Francesco Casella * **Giovanni Mangola** * **Dario Alfani** **

* *Dipartimento di Elettronica, Informazione e Bioingegneria, Politecnico di Milano, Milano, Italy (e-mail: francesco.casella@polimi.it, giovanni.mangola@polimi.it)*
** *Dipartimento di Energia, Politecnico di Milano, Italy (e-mail:dario.alfani@polimi.it)*

Abstract: In this paper, the problem of controlling the thermodynamic state at the outlet of the air cooling unit in a supercritical CO_2 Brayton cycle is addressed. First-principle modelling analysis of the cooler model with boundary conditions representing the interaction with the full plant reveals that the dynamic response of the CO_2 outlet density to small changes of the cooling air flow has a much higher gain and a much more regular behaviour across the whole operating range of the system than the outlet temperature, suggesting to use the former variable for feedback control instead of the latter. Furthermore, it is shown how adaptive density feedback controllers can be designed with simple gain scheduling policies based on the plant load level and on the cooling air temperature.

Keywords: Modeling and simulation of power systems, Control system design, Control of renewable energy sources, Supercritical CO_2 Brayton cycles.

1. INTRODUCTION

Supercritical carbon dioxide (sCO_2) cycles for power generation are likely to play a relevant role in the future energy scenario and, over the past decade, have received increasing attention from industry, research institutions, and academia as demonstrated by the large amount of research effort and investments. Thanks to the potential higher efficiency, the simpler plant arrangement and the faster transients allowed by the more compact turbine, sCO_2 Brayton cycles are commonly identified as the most promising technology to replace conventional steam Rankine cycles in a number of applications as concentrating solar power (CSP) (Binotti et al., 2017), nuclear (Dostal et al., 2004), coal (Alfani et al., 2019a), natural gas and waste heat recovery (WHR) (Astolfi et al., 2018).

Carbon dioxide has a nearly ambient critical temperature, about 31°C, so sCO_2 power cycles take advantage of this property by compressing the carbon dioxide in a region close to the critical point, where the density is much larger than in standard Brayton cycles because of the remarkably low compressibility factor (around 0.2-0.3) of sCO_2 in that region, resulting in much reduced compression work, hence much lower compressor power compared to the turbine power (Angelino, 1969).

Steady-state analysis and design of sCO_2 Brayton cycles always assumes that the main compressor operates with fixed pressure and temperature conditions over the entire operating range of the system, see e.g. (Deshmukh et al., 2019)(Tang et al., 2019)(Moisseytsev et al., 2009)(Moisseytsev and Sienicki, 2011). However, small changes in temperature close to the critical point during plant operation can lead to large changes in the fluid density, significantly affecting the compressor operation and potentially reducing the cycle efficiency.

A robust and fast control system is thus required to keep compressor inlet conditions (corresponding to the cooler outlet conditions in the sCO_2 cycle) constant during load change ramps (Deshmukh et al., 2019). The approach taken so far in the literature is to control the cooler outlet conditions by means of a temperature feedback loop, see, e.g., (Liese et al., 2019).

The large range of possible applications and the possible scarcity of water, coupled to the EU community effort to reduce water consumption, makes the use of direct air-cooled heat rejection units of great interest for sCO_2 systems. On the other hand, the higher variability of ambient air temperature compared to river, lake, or sea water temperature leads to possible issues in the control of the operating conditions at compressor inlet.

This paper thus focuses on the control of the cooling unit in the sCO_2 power cycle, which rejects the low-temperature thermal power to the ambient, assuming the use of an air cooler. The goal of the controller is to maintain the thermodynamic conditions of the fluid at the cooler outlet as close as possible to the required conditions at the main compressor inlet, which are close to the critical point, by modulating the cooling air flow.

The main result of the analysis is that the control of such conditions can be achieved much more effectively by using the fluid density instead of the fluid temperature as the process variable to be controlled in closed loop.

⋆ This research work is supported by the European Commission under Horizon 2020 Grant 764690 - Project sCO2-Flex

Manuscript 2608 submitted to 21st IFAC World Congress, 2020.
Received November 17, 2019.

The paper is organized as follows: in Section 2, a first-principles dynamic model of the process is presented; in Section 3, possible control structures are presented, trying to exploit the specific properties of the process; in Section 4, the results of the analysis are shown, motivating the use of density feedback for the process control. Section 5 concludes the paper with indications for future work.

2. PROCESS MODEL

The present study is motivated by the objective of the Horizon 2020 sCO2-Flex project, which is the full design of a flexible 25 MW_{el} sCO_2 cycle, powered by a coal-fired boiler, or possibly by other sources such as solar power. The process flow diagram is shown in Fig. 1. This paper is focused on the control of the conditions at the cooler (or heat rejection) unit outlet (Fig. 1, bottom left), so the idea is to isolate the cooler from the process, by providing it with simplified boundary conditions that represent the interaction with the rest of the plant, as done in similar studies, e.g. (Liese et al., 2019).

More specifically, the mass flow rate and temperature of CO_2 at the cooler inlet (point 1 in Fig. 1) and the pressure at the cooler outlet (point 2 in Fig. 1) are assumed to have prescribed values, which depend on the load level and are the result of an optimization of plant efficiency for each operating condition, obtained through a numerical code for the sCO2-flex plant steady-state simulation (Alfani et al., 2019b). Different values of the cooling air temperature will also be considered, but as the ambient air temperature changes slowly, the dynamic response to their changes is not of particular interest.

The main assumption, as in similar studies, is that the dynamic response of the thermodynamic conditions at the cooler outlet to changes of the cooling air flow rate of interest is sufficiently decoupled from the other dynamic phenomena taking place in the rest of the plant, so that the indications drawn from the analysis carried out in this paper can also be useful in the context of the full sCO_2 plant control.

The cooler model is a full nonlinear, first-principles model built in Modelica (Mattsson et al., 1998) using the ThermoPower library (Casella and Leva, 2005, 2006) and the ExternalMedia library (Casella and Richter, 2008) for access to sCO_2 fluid properties.

The object diagram of the model, taken from the full sCO2-flex plant model, is shown in Fig. 2: the component at the top describes the mass, momentum, and energy

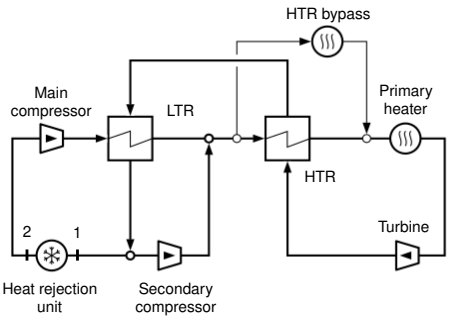

Fig. 1. Process flow diagram of the sCO2-flex plant

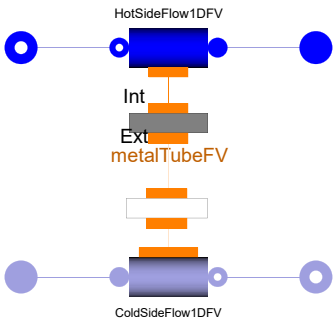

Fig. 2. Modelica diagram of the air cooler model

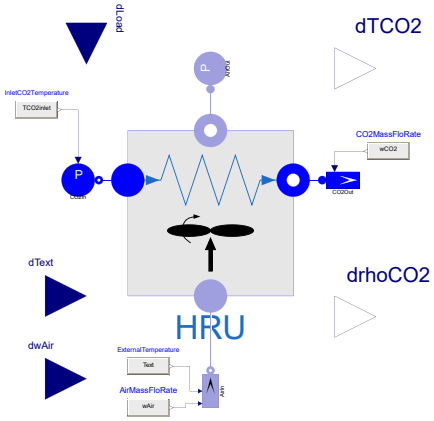

Fig. 3. Modelica diagram of the air cooler fitted with boundary conditions

equations of a 1D, finite-volume model of the CO_2 flow, and the computation of the heat transfer to the tube walls using the well-known Gnielinski correlation. This component exchanges heat through a distributed 1D thermal port with a 1D thermal model of the tube walls, which in turn exchanges heat with a 1D model of the cooling air flow, through a component describing an ideal counter-current heat transfer configuration. The heat transfer coefficient between the cooling air flow and the external wall surface is assumed to be proportional to the mass flow rate to the power of 0.6.

All the 1D models are discretized with 30 finite volumes; note that a quite high number of volumes is necessary to describe the drastic changes of fluid properties along the tube lenght, in particular the specific heat capacity c_p towards the end of the CO_2 tube, where the thermodynamic conditions get closer to the critical point.

The cooler model, a component that will also be used for the modelling of the entire sCO_2 cycle plant of Fig. 1, is then completed by the simplified boundary components, as discussed previously in this Section, and complemented with top-level input and output connectors representing small changes of the inputs and outputs of interest, to be used for the computation of linearized system dynamics and transfer functions, see Fig. 3.

The offset values for CO_2 inlet temperature and mass flow rate, CO_2 outlet pressure, external air temperature and mass flow rate, were all taken from the results of the static

Manuscript 2608 submitted to 21st IFAC World Congress, 2020.
Received November 17, 2019.

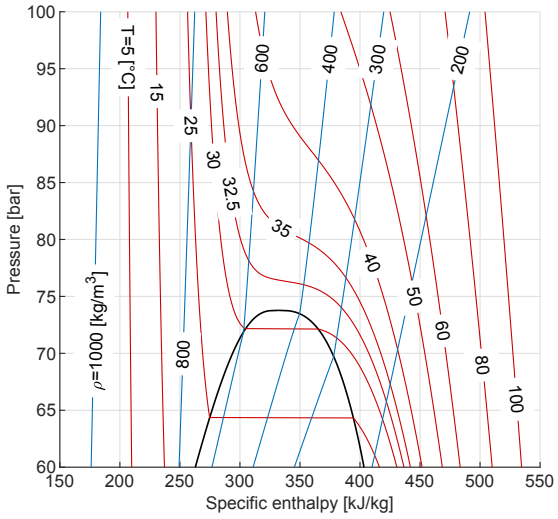

Fig. 4. p-h diagram of the CO_2, obtained trough RefProp 9.1 (Lemmon et al., 2018)

on-design and off-design study that was performed on the sCO2-flex full plant (Alfani et al., 2019b).

Finally, initial equations are added to prescribe steady-state conditions for all state variables, as well as to prescribe the desired CO_2 outlet temperature. The cooling air flow rate offset value is declared as a free parameter, whose value is computed backwards by the Modelica tool to obtain the desired initial CO_2 outlet temperature. In this way, the cooler model can be initialized in steady state operating conditions, corresponding to different load levels of the full sCO_2 plant, and to different external air temperature values.

A final crucial consideration concerns the thermodynamic state at the cooler outlet. As already mentioned in Section 1, the sCO_2 cycle is designed on purpose with the thermodynamic conditions at the main compressor inlet (corresponding to the cooler outlet) close to the critical point, in order to exploit the real gas effect to obtain a high flow density and a corresponding low compression work. However, the thermodynamic behaviour of the fluid in that region is rather peculiar.

When removing thermal power from a fluid in a heat exchanger, the specific enthalpy h is reduced. Looking at the p-h diagram of Fig 4, in the regions to the right and to the left of the saturation dome, that correspond to liquid and superheated vapour or gas, the isothermal curves (in red) are almost vertical, meaning that changes of enthalpy basically correspond to changes of temperature. However, in the region where the cooler outlet operates, which is immediately above the critical point, those curves become almost horizontal instead, meaning that a change of enthalpy doesn't really correspond to a change in temperature. Moreover, the slope of those curves changes dramatically in the neighbourhood of the critical point, suggesting highly nonlinear behaviour of the temperature in that operating region.

If one looks at the isochoric lines (in blue) instead, corresponding to points with the same density, the behaviour in the cooler outlet operating region, slightly above the critical point, turns out to be very regular, with almost vertical lines. This means that in the neighbourhood of the critical point, the fluid density is a much more reliable and much more linear indicator of the enthalpy content of the fluid than the fluid temperature is.

This observation suggest the use of density instead of temperature as a better choice of process variable for feedback control of the cooler outlet state.

3. PROCESS CONTROL STRUCTURES

In the context of the simplified process structure described in the previous section, four simple controller structures can be considered. The simplest possible ones are feedback control of cooler outlet temperature and feedback control of cooler outlet density, as shown in Fig 5.a-b. In the second case, the density must be measured directly, using sensors based on the Coriolis effect (Morris and Langari, 2016). In all cases, the cooling air mass flow rate, which is roughly proportional to the cooling fan speed, is used as the manipulated variable of the process.

Considering that the original sCO_2 power cycle which motivates this study is designed to work in the 20%–100% load range, one can expect a significant variation of the dynamic response of the process seen by the controller between the full-load case and the minimum-load case. One could then think of compensating this variation by introducing a simple form of gain scheduling, e.g., multiplying the controller output by the load level in p.u., as shown in Fig. 5.c-d.

It is then possible to assess which of the four proposed controller structures is the most effective one by evaluating the frequency response between small variations of the output u of the controller block C (before the multiplication node in the last two cases) and the corresponding variations of the process output T_{out} or ρ_{out}.

4. RESULTS OF THE ANALYSIS

The analysis proposed in Section 3 was carried out on the process model presented in Section 2. The Modelica tool Dymola was used to compute the steady-state operating conditions of the cooler corresponding to different load levels of the original sCO_2 power cycle, considering the design value of the cooling air, 20 °C. Then, the tool was used to compute linearized models at those equilibrium conditions, from which the frequency response of the transfer functions between small changes of the cooling air mass flow rate and the temperature and density at the cooler outlet were obtained.

The obtained frequency responses, which correspond to the dynamic behaviour seen by the controller C in Fig. 5.a-b, turn out to be heavily affected by the load level, with changes of the static gain up to a factor five; hence, they are not particularly favourable for the design of the controller C, and thus not reported here due to space limitations.

The frequency responses of the transfer functions multiplied by the load level, which correspond to the dynamic behaviour seen by the feedback controller C in Fig. 5.c-d,

Manuscript 2608 submitted to 21st IFAC World Congress, 2020.
Received November 17, 2019.

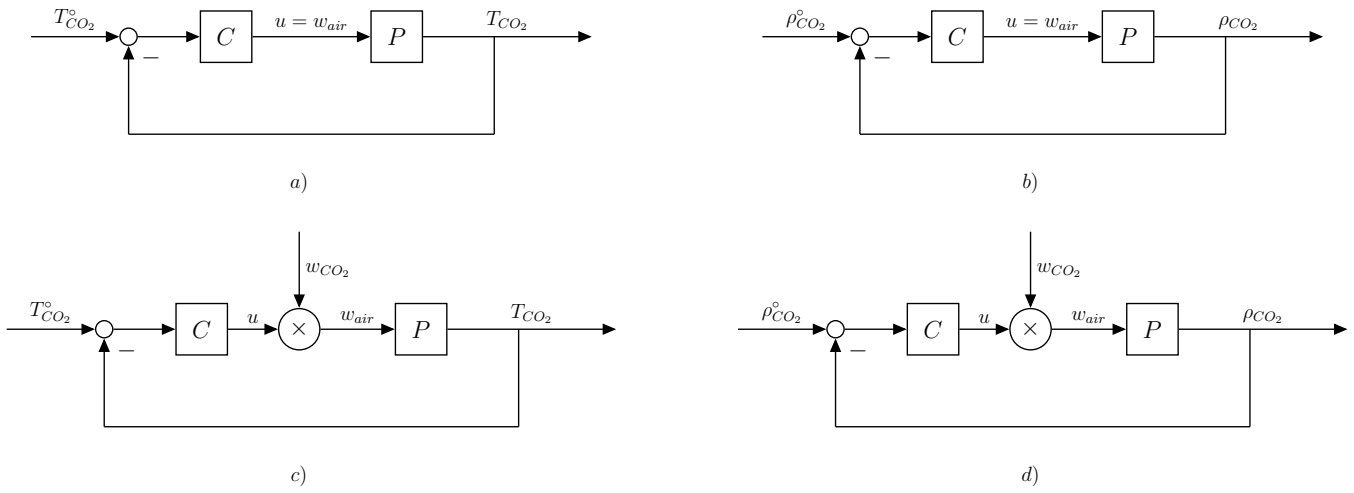

Fig. 5. Alternative process control structures

are instead shown in Fig. 6. All variables have been normalized: the cooling air flow and the outlet fluid density are divided by their design value, while the outlet temperature is divided by the difference between cooler inlet and outlet temperature in design conditions.

The first important outcome is that the gain of the normalized transfer function is one order of magnitude higher in the case of the density feedback than in the case of the temperature feedback. This means that temperature controllers need to have much higher gains than density controllers, leading to much higher sensitivity to sensor noise.

For example, looking at the static gains of the transfer functions, a variation of 1% of the air flow rate corresponds to a change of 3.6 kg/m^3 in the cooler outlet density, which is about 0.4% of the measurement range 0–1000 kg/m^3 of the corresponding sensor, while it corresponds to a change of a meager 0.07 K of the outlet temperature, which is only 0.07% of the range of a temperature sensor calibrated in the range 0–100°C. It then apparent how temperature feedback controllers will be a lot more critical from the point of view of sensor signal/noise ratio and of sensitivity to sensor noise than density feedback controllers.

Additionally, the temperature measurement may also be affected by significant additional phase lag due to the temperature sensor inertia, which is not the case for the much faster density sensor.

The second important result is that the dynamic behaviour of the density response, once corrected by the load level, is only marginally affected by the load level itself, as is apparent from the fact that the Bode plots computed at different load levels are very close to each other. Conversely, despite the load correction, the gain of the transfer function to the temperature decreases by a factor five when the load is reduced from 100% to 45%, and then increases again by a factor three when the load is further reduced to 20%.

This means that a fixed-parameter density controller C used in the structure of Fig. 5.d can be designed to obtain good performance over the entire operating range of the plant, while some kind of much more involved adaptive or gain-scheduling controller C would be required for the temperature feedback structure of Fig. 5, bottom-left.

Notice how these conclusions can be drawn from the analysis of the process dynamics, regardless of the actual design and implementation of the controller C.

To complete the analysis, the effect of changes in the steady-state value of the cooling air temperature was analyzed. A reduction of the air temperature from the design value of 20 °C down to -5°C changes the gain of the transfer function seen by block C in Fig. 3.d very significantly. This can be easily explained, since a larger temperature difference between the cooling air and the CO_2 means that the same increase in air flow carries away more heat, thus increasing the transfer function gain.

However, if another multiplicative compensation by the factor $1/\Delta T$ is added at the controller output, where ΔT is the difference between the cooler outlet desired temperature and the cooling air temperature (see Fig. 7), the resulting transfer functions seen by the C controller have the frequency responses shown in Fig. 8, which are fairly insensitive to changes in both load level and external air temperature, except for the cases of low load and low external temperature.

Based on this result, if the control architecture of Fig. 7 is used, a fixed-parameter C controller is easily designed to cope with loads between 100% and about 50% and air temperatures between 20 °C and about 5°C. Handling the more extreme conditions may require either some more sophisticated gain scheduling policy, or the use of a robust controller for the C block, that can manage the reduced magnitude and added phase lag in those conditions. Note that the reduction of the frequency response magnitude at low load and external temperature when using a fixed-parameter C block causes a reduction of the crossover frequency that will recover some of the lost phase margin, at the cost of a reduced controller bandwidth, which may be acceptable when operating close to the minimum load of the plant.

Last, but not least, note that the gain scheduling signals in Fig. 7 depend on exogenous disturbances (external air

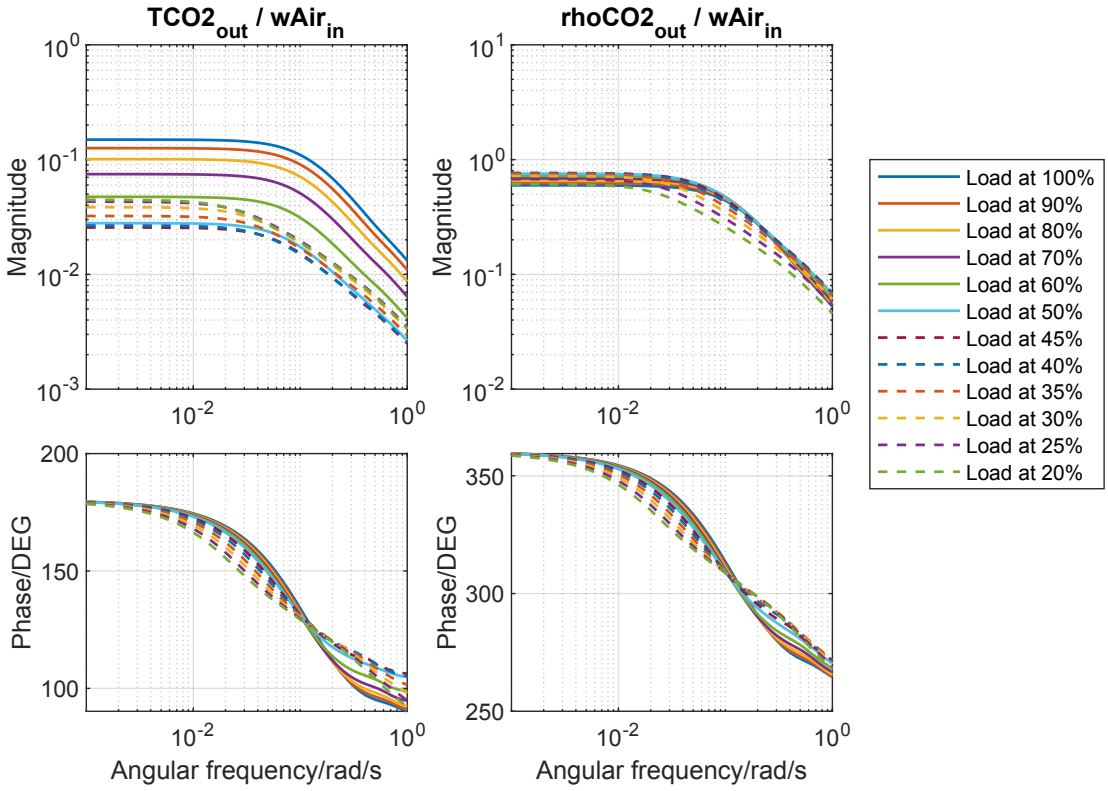

Fig. 6. Frequency responses of the process as seen by blocks C in Fig. 5.c-d – normalized units

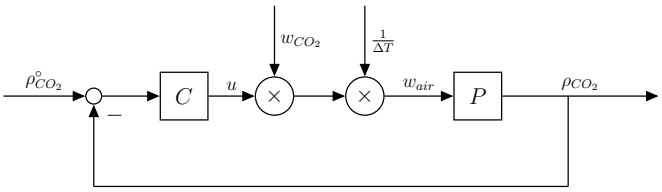

Fig. 7. Density feedback control with load and ΔT gain scheduling

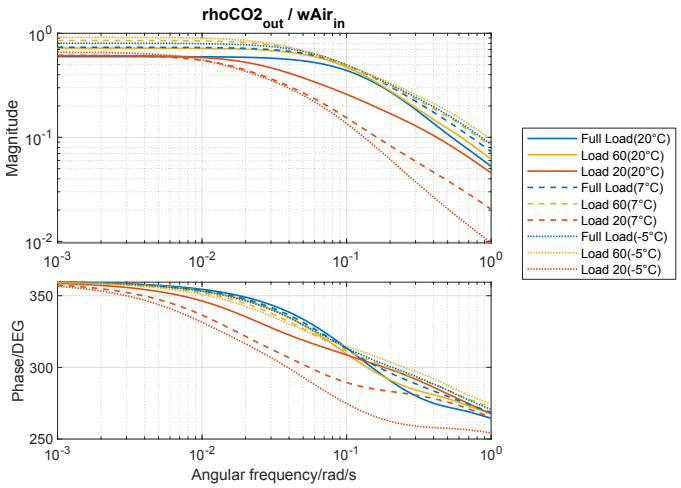

Fig. 8. Frequency response of the process as seen by block C in Fig. 7 – normalized units

temperature) and set points (load, desired cooler outlet temperature), so that there are no stability issues due to parasite nonlinear feedback loops enabled by the gain-scheduling policy.

Summing up, compared to the conventional choice of temperature feedback, the use of cooler outlet density as a feedback variable provides higher process gain and signal-to-noise ratio, and makes it simpler to manage the variability of the process small signal response due to the load and external temperature variations. It is expected that this will also be the case when considering plant-wide control of the full sCO_2 cycle of Fig. 1.

5. CONCLUSIONS AND FUTURE WORK

In this paper, the process dynamics of the air cooler in a sCO_2 power cycle was analyzed by means of a nonlinear first-principle model of the cooler, neglecting the dynamic interaction with the rest of the plant, which is described by representative boundary conditions, while still taking into account the operating conditions of the full plant in the range $20\% - 100\%$ of the design load.

The analysis of the process dynamics, which is also motivated by the thermodynamic behaviour of sCO_2 close to the critical point, suggests that the thermodynamic state of the fluid at the cooler outlet is more effectively and more easily controlled if the cooler outlet density is used for feedback, instead of the cooler outlet temperature; the density can be measured directly with Coriolis-force based sensors. Furthermore, the addition of a simple gain scheduling poli-

Manuscript 2608 submitted to 21st IFAC World Congress, 2020.
Received November 17, 2019.

cies, based on the load level and on the difference between the desired CO_2 outlet temperature and the cooling air temperature, dramatically reduces the variability of the process seen by the feedback controller, facilitating the design of simple gain-scheduling controllers.

These ideas will be used when tackling the plant-wide control problem of the full sCO_2 power cycle, which is currently under evaluation, and are expected to provide useful indications also in that more general case.

The authors also believe that density-based control will also be more effective than temperature-based control in case a water cooler is used, since the nonlinear behaviour of sCO_2 is not really affected by the type of fluid used on the cold side of the heat exchanger, while the influence of the cooling medium temperature will be less important, since the variability of cooling water supply temperatures is much lower than that of ambient air.

REFERENCES

Alfani, D., Astolfi, M., Binotti, M., Campanari, S., Casella, F., and Silva, P. (2019a). Multi Objective Optimization of Flexible Supercritical CO2 Coal-Fired Power Plants. volume Volume 3: Coal, Biomass, Hydrogen, and Alternative Fuels; Cycle Innovations; Electric Power; Industrial and Cogeneration; Organic Rankine Cycle Power Systems of *Turbo Expo: Power for Land, Sea, and Air*. doi:10.1115/GT2019-91789. URL `https://doi.org/10.1115/GT2019-91789`. V003T06A027.

Alfani, D., Astolfi, M., Binotti, M., Macchi, E., and Silva, P. (2019b). Part-Load Operation Of Coal Fired sCO2 Power Plants. In *3rd European supercritical CO2 Conference September 19-20, 2019, Paris, France*, 1–9.

Angelino, G. (1969). Real gas effects in carbon dioxide cycles. Technical report. doi:10.1115/69-GT-102. URL `http://www.asme.org/about-asme/terms-of-use`.

Astolfi, M., Alfani, D., Lasala, S., and Macchi, E. (2018). Comparison between ORC and CO2 power systems for the exploitation of low-medium temperature heat sources. *Energy*, 161, 1250–1261. doi:10.1016/J.ENERGY.2018.07.099. URL `https://www.sciencedirect.com/science/article/pii/S0360544218313963?via{\%}3Dihub`.

Binotti, M., Astolfi, M., Campanari, S., Manzolini, G., and Silva, P. (2017). Preliminary assessment of sCO2 cycles for power generation in CSP solar tower plants. *Applied Energy*, 204, 1007–1017. doi:10.1016/j.apenergy.2017.05.121. URL `http://dx.doi.org/10.1016/j.apenergy.2017.05.121`.

Casella, F. and Leva, A. (2005). Object-oriented modelling & simulation of power plants with modelica. In *Proceedings 44th IEEE Conference on Decision and Control and European Control Conference 2005*, 7597–7602. IEEE, EUCA, Seville, Spain.

Casella, F. and Leva, A. (2006). Modelling of thermo-hydraulic power generation processes using Modelica. *Mathematical and Computer Modeling of Dynamical Systems*, 12(1), 19–33. doi:10.1080/13873950500071082.

Casella, F. and Richter, C.C. (2008). ExternalMedia: a library for easy re-use of external fluid property code in Modelica. In B. Bachmann (ed.), *Proceedings 6th International Modelica Conference*, 157–161. Modelica Association, Bielefeld, Germany. URL `http://www.modelica.org/events/modelica2008/Proceedings/sessions/session2b1.pdf`.

Deshmukh, A., Kapat, J., and Khadse, A. (2019). Transient Thermodynamic Modeling of Air Cooler in Supercritical CO2 Brayton Cycle for Solar Molten Salt Application. volume Volume 9: Oil and Gas Applications; Supercritical CO2 Power Cycles; Wind Energy of *Turbo Expo: Power for Land, Sea, and Air*. doi:10.1115/GT2019-91409. URL `https://doi.org/10.1115/GT2019-91409`. V009T38A023.

Dostal, V., Driscoll, M., and Hejzlar, P. (2004). A Supercritical Carbon Dioxide Cycle for Next Generation Nuclear Reactors. *Technical Report MIT-ANP-TR-100*, 1–317. doi:MIT-ANP-TR-100.

Lemmon, E.W., , Bell, I.H., Huber, M.L., and McLinden, M.O. (2018). NIST Standard Reference Database 23: Reference Fluid Thermodynamic and Transport Properties-REFPROP, Version 9.1, National Institute of Standards and Technology. doi:http://dx.doi.org/10.18434/T4JS3C. URL `https://www.nist.gov/srd/refprop`.

Liese, E., Mahapatra, P., and Jiang, Y. (2019). Modeling and Control of a Supercritical CO2 Water Cooler in an Indirect-Fired 10MWe Recompression Brayton Cycle Near Critical Conditions. volume Volume 9: Oil and Gas Applications; Supercritical CO2 Power Cycles; Wind Energy of *Turbo Expo: Power for Land, Sea, and Air*. doi:10.1115/GT2019-90496. URL `https://doi.org/10.1115/GT2019-90496`. V009T38A009.

Mattsson, S.E., Elmqvist, H., and Otter, M. (1998). Physical system modeling with Modelica. *Control Engineering Practice*, 6(4), 501–510.

Moisseytsev, A., Kulesza, K.P., Sienicki, J.J., Division, N.E., and Univ., O.S. (2009). Control system options and strategies for supercritical co2 cycles. doi:10.2172/958037.

Moisseytsev, A. and Sienicki, J.J. (2011). Development of the anl plant dynamics code and control strategies for the supercritical carbon dioxide brayton cycle and code validation with data from the sandia small-scale supercritical carbon dioxide brayton cycle test loop. doi:10.2172/1040687.

Morris, A.S. and Langari, R. (2016). Chapter 16 - flow measurement. In A.S. Morris and R. Langari (eds.), *Measurement and Instrumentation (Second Edition)*, 493 – 529. Academic Press, Boston, second edition edition. doi:https://doi.org/10.1016/B978-0-12-800884-3.00016-2. URL `http://www.sciencedirect.com/science/article/pii/B9780128008843000162`.

Tang, C.J., McClung, A., Hofer, D., and Huang, M. (2019). Transient Modeling of 10 MW Supercritical CO2 Brayton Power Cycles Using Numerical Propulsion System Simulation (NPSS). volume Volume 9: Oil and Gas Applications; Supercritical CO2 Power Cycles; Wind Energy of *Turbo Expo: Power for Land, Sea, and Air*. doi:10.1115/GT2019-91443. URL `https://doi.org/10.1115/GT2019-91443`. V009T38A024.

Manuscript 2608 submitted to 21st IFAC World Congress, 2020.
Received November 17, 2019.